Carbohydrate Polymers 121 (2015) 388–402

Contents lists available at ScienceDirect

Carbohydrate Polymers

journal homepage: www.elsevier.com/locate/carbpol

Activation of RAW264.7 macrophages by the polysaccharide from the roots of *Actinidia eriantha* and its molecular mechanisms

Hongxiang Sun[a,*], Juan Zhang[a], Fengyang Chen[a,b], Xiangfeng Chen[a], Zhihua Zhou[a], Hui Wang[a]

[a] Key Laboratory of Animal Virology of Ministry of Agriculture, College of Animal Sciences, Zhejiang University, Hangzhou 310058, China
[b] Institute of Materia Medica, Zhejiang Academy of Medical Sciences, Hangzhou 310013, China

ARTICLE INFO

Article history:
Received 29 November 2013
Received in revised form 8 October 2014
Accepted 3 December 2014
Available online 3 January 2015

Keywords:
Actinidia eriantha
Polysaccharides
RAW264.7 cell
Toll-like receptor (TLR)
NF-κB signaling pathway
PCR array

ABSTRACT

The polysaccharide from the roots of *Actinidia eriantha* (AEPS), a potent antitumor agent and immunological adjuvant, was investigated for the immunomodulatory effects on RAW264.7 macrophages and its molecular mechanisms. AEPS could significantly enhance the pinocytic and phagocytic activity, induce the production of NO, TNF-α, IL-10, IL-1β and IL-6, and promote the expression of accessory and costimulatory molecules in RAW264.7 cells. PCR array assay revealed that AEPS up-regulated 28 genes including TLRs (TLR2, TLR8, TLR9), proinflammatory factors (IL-1β, G-CSF, IL-1α, GM-CSF, IL-6, COX-2, TNF-α, IFN-β, CXCL10, CCL2, TNF-β, IL-10), and the genes involved in NF-κB signaling pathway, and down-regulated 6 genes such as TLR3, TLR4, PGLYRP1, EIF2αK2, MAP3K1 and IRF1. AEPS was further showed to promote cytoplasmic IκB-α degradation and increase nuclear NF-κB p65 levels in RAW264.7 cells. These results suggested that AEPS activated RAW264.7 macrophages and elicited a M1 and M2 response through TLRs/NF-κB signaling pathway.

1. Introduction

Polysaccharides obtained from natural sources represent a structurally diverse class of macromolecules, and are known to affect a variety of biological responses, especially the immune response. Most polysaccharides derived from higher plants are relatively nontoxic and do not cause significant side effects, which is a major problem associated with bacterial polysaccharides and synthetic compounds. The plant polysaccharides are recognized as an effective biological response modifier with low toxicity (Petrovsky & Cooper, 2011). Recently, many polysaccharides have been shown to possess adjuvant potential on specific cellular and humoral immune responses against antigen, and be excellent adjuvant candidates for many vaccines (Licciardi & Underwood, 2011). Thus, the plant polysaccharides have enormous potential for use as an adjuvants in vaccines against both pathogens and cancer (Granell, Fernández-del-Carmen, & Orzáez, 2010).

The roots of *Actinidia eriantha* Benth (Actinidiaceae) have been used for gastric carcinoma, nasopharyngeal carcinoma, breast carcinoma, and hepatitis in traditional Chinese medicine. The modern pharmacological experiments proved that the water extracts of this drug possessed antitumor and immunopotentiating activities. In our previous works, the polysaccharide from the roots of *A. eriantha* (AEPS) has been shown to be the main active principles responsible for the antitumor and immunomodulatory effect of this drug (Xu, Yao, Sun, & Wu, 2009). AEPS was also proved to possess the immunological adjuvant activity on specific cellular and humoral immune responses to ovalbumin (OVA) in mice, and elicit a Th1 and Th2 immune responses (Sun, Wang, Xu, & Ni, 2009). Moreover, its low toxicity, no side effects and availability all make it as a safe and efficacious adjuvant candidate suitable for a wide spectrum of prophylactic and therapeutic vaccines. However, the underlying mechanisms of AEPS in the regulation of immune response need to be investigated.

Macrophages occupy a unique niche in the immune system, in that they can not only initiate innate immune responses, but also be effector cells that contribute to fight infection and inflammation. Macrophages can kill pathogens directly by phagocytosis and indirectly via the secretion of pro-inflammatory factors. Macrophages also exert an important role as an interface between innate and adaptive immunity. They are responsible for processes such as antigen processing and presentation to antigen-specific T cells. Following activation, macrophages can induce expression of accessory and costimulatory molecules that promote sustained stimulatory interactions with T cells and the generation of adaptive immunity. Indeed, the basic mechanisms of the immunostimulatory,

* Corresponding author. Tel.: +86 571 8898 2091; fax: +86 571 8898 2091.
E-mail address: sunhx@zju.edu.cn (H. Sun).

http://dx.doi.org/10.1016/j.carbpol.2014.12.023
0144-8617/

anti-tumor, bactericidal and other therapeutic effects of plant polysaccharides are thought to occur via activation of immune cells resulting in the induction of immune responses (Beutler, 2004). Macrophages were thought to be the important target cells of some antitumor and immunomodulatory drug (Cheng, Wan, Wang, Jin, & Xu, 2008).

RAW264.7 cells are commonly accepted as a tool to investigate the molecular mechanisms of macrophages involved in regulating immunity (Hartley et al., 2008). The current experiments were designed to investigate the immunomodulatory effects of AEPS on RAW264.7 macrophages by determining the effect on the production and expression of nitric oxide, cytokines, chemokines, accessory and costimulatory molecules, and explore its molecular mechanisms using a high-throughput mouse Toll-like receptor (TLR) signaling pathway PCR array.

2. Materials and methods

2.1. Materials

3-(4,5-Dimethylthiazol-2-yl)-2,5-diphenyltetrazolium bromide (MTT), lipopolysaccharide (LPS), and polymyxin B (PMB) were purchased from Sigma Chemical Co., Saint Louis, MO, USA; DMEM medium was from Gibco, NY, USA. Griess reagent was purchased from Sigma-Aldrich (NSW, Australia). Mouse TNF-α, IL-1β, IL-6 and IL-10 detecting ELISA kits were from Wuhan Boster Biological Technology Co. Ltd., Hubei, China. Trizol was purchased from Invitrogen, USA; revert Aid™ M-MuLV reverse transcriptase was from Fermentas, USA; diethylpyrocarbonate (DEPC), ribonuclease inhibitor and oligo(dT)$_{18}$ were from Sangon, Shanghai, China. RT^2 Profiler™ Mouse Toll-like receptor signaling pathway PCR array (PAMM-053A) was purchased from SABioscience Corp., Frederick, MD, USA. NE-PER® Nuclear and cytoplasmic extraction reagents and BCA™ protein assay kit were purchased from Pierce, Rockford, IL, USA. Fluorescein isothiocyanate (FITC)-conjugated anti-mouse CD40 (Clone: HM40-3), CD80 (Clone: 16-10A1), CD86 (Clone: GL1), MHC-I (H-2Db, Clone: 28-14-8), and MHC-II (I-A/I-E, Clone: M5/114.15.2) monoclonal antibodies (mAbs) were purchased from eBioscience, Inc., San Diego, CA, USA. Monoclonal antibody against actin and polyclonal antibodies (Abs) against IκB-α (Ser32) and NF-κB p65 (Ser536) were from Cell Signaling Technology, Beverly, MA, USA. The enhanced chemiluminescence (ECL) kit was purchased from Amersham Life Science, Amersham, UK, USA; X-ray films were from Kodak, Rochester, NY, USA. PDTC (Ammonium pyrrolidine dithiocarbamate, a NF-κB inhibitor) was from Beyotime, Jiangsu, China. Fetal calf serum (FCS) was provided by Hyclone, Utah, USA.

AEPS was a water-soluble total polysaccharide from the roots of *A. eriantha*, and composed of rhamnose (3.18 mol.%), fucose (14.85 mol.%), arabinose (26.87 mol.%), xylose (4.49 mol.%), mannose (7.83 mol.%), glucose (7.72 mol.%), and galactose (35.05 mol.%) with the molar ratio of 1.00:4.67:8.45:1.41:2.46:2.43:11.02 (Sun et al., 2009). A stock AEPS solution with a concentration of 10 mg/ml was prepared by dissolving in 0.89% saline. The solution was sterilized by passing it through a 0.22-μm Millipore filter, and then analyzed for endotoxin level by a gel-clot *Limulus* amebocyte lysate assay. For further ruling out the possibility of LPS contamination, diluted AEPS solutions were preincubated with polymyxin B (20 μg/ml) for 30 min at room temperature.

2.2. Cell culture

RAW264.7 macrophages were purchased from ATCC (American Type Tissue Culture Collection), and maintained in a 5% CO_2 atmosphere in DMEM medium supplemented with 10% FCS, 50 μM mercaptoethanol, 20 mM HEPES, 10 mM sodium pyruvate, 100 μg/ml streptomycin, and 100 U/ml penicillin.

2.3. Cell viability assay

The effect of AEPS on the viability of RAW264.7 cells was determined by MTT method. RAW264.7 cells were seeded at 2×10^4 cells/well in a 96-well plate and incubated at 37 °C in a humidified atmosphere with 5% CO_2. After 24 h, the various concentrations of AEPS were added into each well and these cells were incubated at 37 °C for 24 h. Each concentration was repeated four wells. 4 h prior to incubation end, 50 μl of MTT solution (2 mg/ml) were added to each well. The plates were further incubated for 4 h, and then centrifuged ($1400 \times g$, 5 min). The untransformed MTT was removed carefully by pipetting. To each well 150 μl of a DMSO solution was added, and the absorbance was evaluated in an ELISA reader at 570 nm with a 630 nm reference after 15 min.

2.4. Pinocytic activity assay

RAW264.7 cells were seeded at 1×10^4 cells/well in a 96-well plate and incubated at 37 °C in a humidified atmosphere with 5% CO_2. After 24 h, DMEM medium, LPS, or the various concentrations of AEPS were added into each well, and these cells were incubated at 37 °C for 24 h. Each concentration was repeated four wells. Culture media were removed and 100 μl/well of 0.075% neutral red was added, and incubated for 30 min. After washed with PBS for three times, 150 μl of cell lyzing solution were added into each well and cells were cultured at 37 °C for 1 h. The absorbance was evaluated in an ELISA reader at 570 nm.

2.5. Determination of phagocytic uptake

After 24 h treated with the various concentrations of AEPS, RAW264.7 cells were harvested and resuspended in 100 μl FITC-labeled dextran (1 mg/ml) and incubated at 37 °C for 30 min. Phagocytosis was then stopped by the addition of 2 ml of ice-cold PBS, and then the cells were washed three times with cold PBS. Flow cytometric analysis was performed using a FACScan flow cytometer using CellQuest software (BD Biosciences, San Jose, CA, USA).

2.6. NO production

After 24 h treated with the various concentrations of AEPS, the culture supernatants of RAW264.7 cells were collected and nitrite contents were determined by Griess reaction. Briefly, 100 μl aliquots of the supernatant were distributed in a 96-well plate and then equal volumes of the Griess reaction solutions (1% sulfanilamide, 0.1% *N*-(1-naphthyl)-ethylenediamine dihydro-chloride in 2.5% phosphoric acid) were added. The reaction was allowed to proceed for 10 min at room temperature. The absorbance was read at 540 nm, and the concentrations of NO_2^- were determined from a least squares linear regression analysis of a sodium nitrite standard curve.

2.7. Cytokine assays

The culture supernatants of RAW264.7 cells treated with AEPS for 24 h were collected for the detection of TNF-α, IL-1β, IL-6 and IL-10 levels using commercial ELISA kits. The culture supernatants or cytokine standards were added to 96-well plates coated with coating antibody, and plates then incubated at 37 °C for 1.5 h. Plates were washed and a detecting antibody was added to each well. Plates were incubated at 37 °C for 1 h before addition of avidin–biotin–peroxidase complex (ABC). After incubation for 30 min, plates were washed and developed with tetramethyl

benzidine (TMB) at 37 °C for 15 min. The reaction was stopped by addition of 100 μl of stop solution. The absorbance was measured in an ELISA reader at 450 nm. The concentrations of TNF-α, IL-1β, IL-6 and IL-10 were calculated according to the standard curve using each of the recombinant cytokines in the ELISA kits.

2.8. Flow cytometry

The detection of accessory and costimulatory molecule expression on RAW264.7 cells was performed by flow cytometer. RAW264.7 cells treated with AEPS for 24 h were harvested and washed with PAB (1% bovine serum albumin and 0.1% sodium azide in PBS). Cells were blocked with 1 μg of purified anti-mouse CD16/CD32 antibody (FcR block) for 10 min to inhibit non-specific staining, and then stained with optimal concentrations of FITC-conjugated anti-mouse CD40, CD80, CD86, MHC-I and MHC-II antibodies for an additional 30 min. Parallel sets of cells were incubated with monoclonal immunoglobulin isotypes, and the fluorescence intensity of these cells served as non-specific negative control. One hundred thousand viable cells per treatment (as determined by light scatter profiles) were analyzed using a BD FACScan flow cytometer using CellQuest software.

2.9. RT-PCR analysis

After incubation with or without AEPS, RAW264.7 cells were subjected to Trizol reagent and the total RNA was isolated according to the manufacture's protocol, and reverse transcription was performed as previously (Sun et al., 2009). Then amplification was carried out in a total volume of 20 μl containing 0.5 μl (20 μM) of each specific primer, 2 μl of 10× PCR buffer, 1.2 μl of $MgCl_2$ (25 mM), 0.5 μl of dNTP (10 mM), 1 μl of transcribed cDNA, and 0.25 μl of Taq DNA polymerase. PCR was performed for multiple cycles using a PTC-200 thermal cycler (Bio-Rad Laboratories, Inc., USA) with the following program of denaturation at 94 °C for 1 min, annealing for 50 s, and elongation at 72 °C for 0.5 min. The specific primers, amplified cycles and annealing temperature of each tested gene were listed in Supplementary Table S1. Semi-quantitative RT-PCR was performed using GAPDH as an internal control to normalize gene expression for the PCR templates. The PCR products were analyzed by electrophoresis on a 1.5% agarose gel containing goldview (5 μl/100 ml), and the amplified bands were visualized and photographed using JS-680B Gel Documentation and Analysis System (Shanghai Peiqing Science and Technology Co., Ltd, China). The size of the amplified fragments was determined by comparison with a standard DNA marker.

2.10. PCR array analysis

The RT^2 *Profiler*™ Mouse Toll-like receptor signaling pathway PCR array (PAMM-053A) was used to analyze the mRNA expression levels of 84 genes related to TLR-mediated signal transduction in RAW264.7 cells treated with AEPS for 3 h. Quality control of RNA samples, synthesis of cDNA, and real-time RT-PCR arrays were performed as described (Chen et al., 2012; Wang, Chen, Zhou, Li, & Sun, 2013). All genes represented by the array showed a single peak on the melting curve characteristic to the specific products. Data analysis of gene expression was performed using Excel-based PCR Array Data Analysis Software provided by manufacturer (Qiagen). Fold-changes in gene expression were calculated using the $\Delta\Delta Ct$ method, and five stably expressed housekeeping genes β-glucuronidase (GUSB), hypoxanthine guanine phosphoribosyl transferase 1 (HPRT1), Heat shock protein 90 α (cytosolic), class B member 1 (HSP90AB1), GAPDH, and β-actin were used for normalization of the results.

2.11. Western blot analysis

After treated with the various concentrations of AEPS for 30 min, RAW264.7 cells were washed twice with cold PBS and lysed with NE-PER™ nuclear and cytoplasmic extraction reagents (Pierce, Rockford, IL, USA). The protein contents were measured with the BCA protein assay kit using bovine serum albumin as a standard. The denatured proteins were separated on 10–12% sodium dodecyl sulfate polyacrylamide gel electrophoresis (SDS-PAGE), and transferred to PVDF membrane. After blocking the membrane with 5% skim milk in Tween-20 containing Tris buffered saline (TTBS) (20 mM Tris–HCl (pH 7.6), 150 mM NaCl, 0.1% Tween-20) for 2 h at 37 °C, the blot was incubated with rabbit monoclonal antibody I-κBα and p65 NF-κB (1:1000), and mouse monoclonal antibody anti-Actin in TTBS containing 5% skim milk overnight at 4 °C. Subsequently, the membranes were washed with TTBS and incubated with an appropriate secondary antibody (horseradish peroxidase-conjugated goat anti-mouse or anti-rabbit IgG) for 2 h. After washing the membrane with TTBS three times for 5 min, the signal was visualized with ECL Detection Kit and exposed the membranes to X-ray films. The bands were visualized and photographed using JS-680B Gel Documentation and Analysis System.

2.12. Statistical analysis

Data were expressed as mean ± SD and examined for their statistical significance of difference with ANOVA and a Tukey post-hoc test. *P*-value less than 0.05 were considered to be statistically significant.

3. Results

3.1. Effects of AEPS on RAW264.7 cell viability

To investigate the effects of AEPS on the growth of RAW264.7 cells, after treated with AEPS (0–100 μg/m1) for 24 h, cells were detected for the viability using MTT assay. As shown in Fig. 1A, AEPS was not cytotoxic to RAW264.7 cells up to the concentration of 200 μg/ml, even promote the cell proliferation at the concentration of 25–100 μg/ml ($P < 0.01$).

3.2. AEPS increased the pinocytic and phagocytic activity of RAW264.7 cells

The effect of AEPS on the pinocytic activity of RAW264.7 cells was examined by the uptake of neutral red. As shown in Fig. 1B, AEPS significantly enhanced the pinocytic activity of RAW264.7 cells in a dose-dependent manner ($P < 0.001$). Meanwhile, we also determined the effect of AEPS on phagocytic uptake of FITC-labeled dextran in RAW264.7 cells using flow cytometer. The fluorescence intensity in RAW264.7 cells was markedly increased by AEPS (Fig. 1C), suggesting that AEPS promote the phagocytic capacities of macrophages.

3.3. AEPS induced the production of NO from RAW264.7 cells

As shown in Fig. 2, a minimum amount of NO was released when RAW264.7 cells were exposed to medium alone, whereas incubation of these cells with increasing amounts of AEPS was associated with a concentration-dependent increase in NO production ($P < 0.001$), suggesting that AEPS significantly induced the production of NO from RAW264.7 cells in a dose-dependent manner.

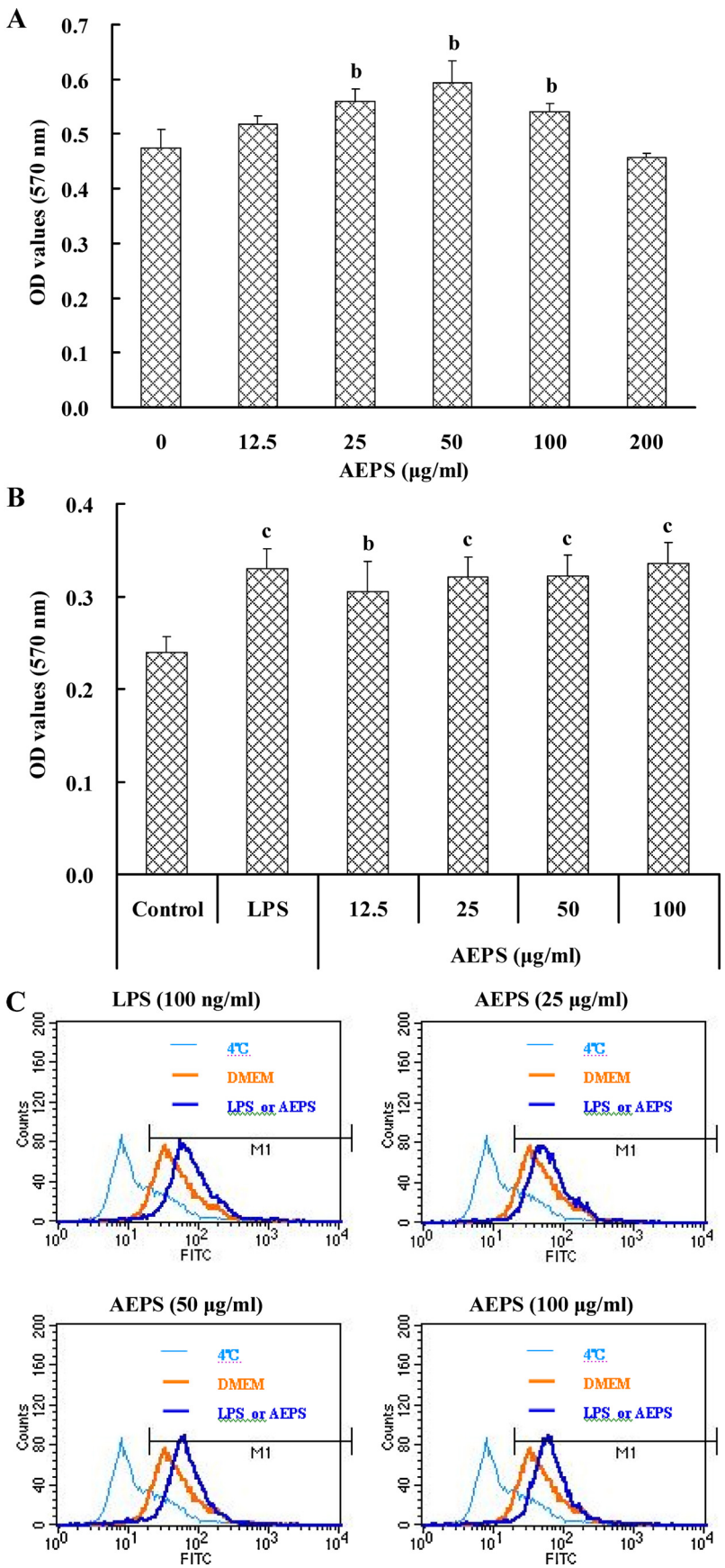

Fig. 1. Effect of the polysaccharide from the roots of *Actinidia eriantha* (AEPS) on viability (A), pinocytic (B) and phagocytic activity (C) of RAW264.7 cells. RAW264.7 cells were treated with AEPS at the various concentrations for 24 h. The values are presented as mean ± SD ($n = 3$). Significant differences with control cells were designated as [b] $P < 0.01$ or [c] $P < 0.001$. The figure shown is representative of three independent experiments.

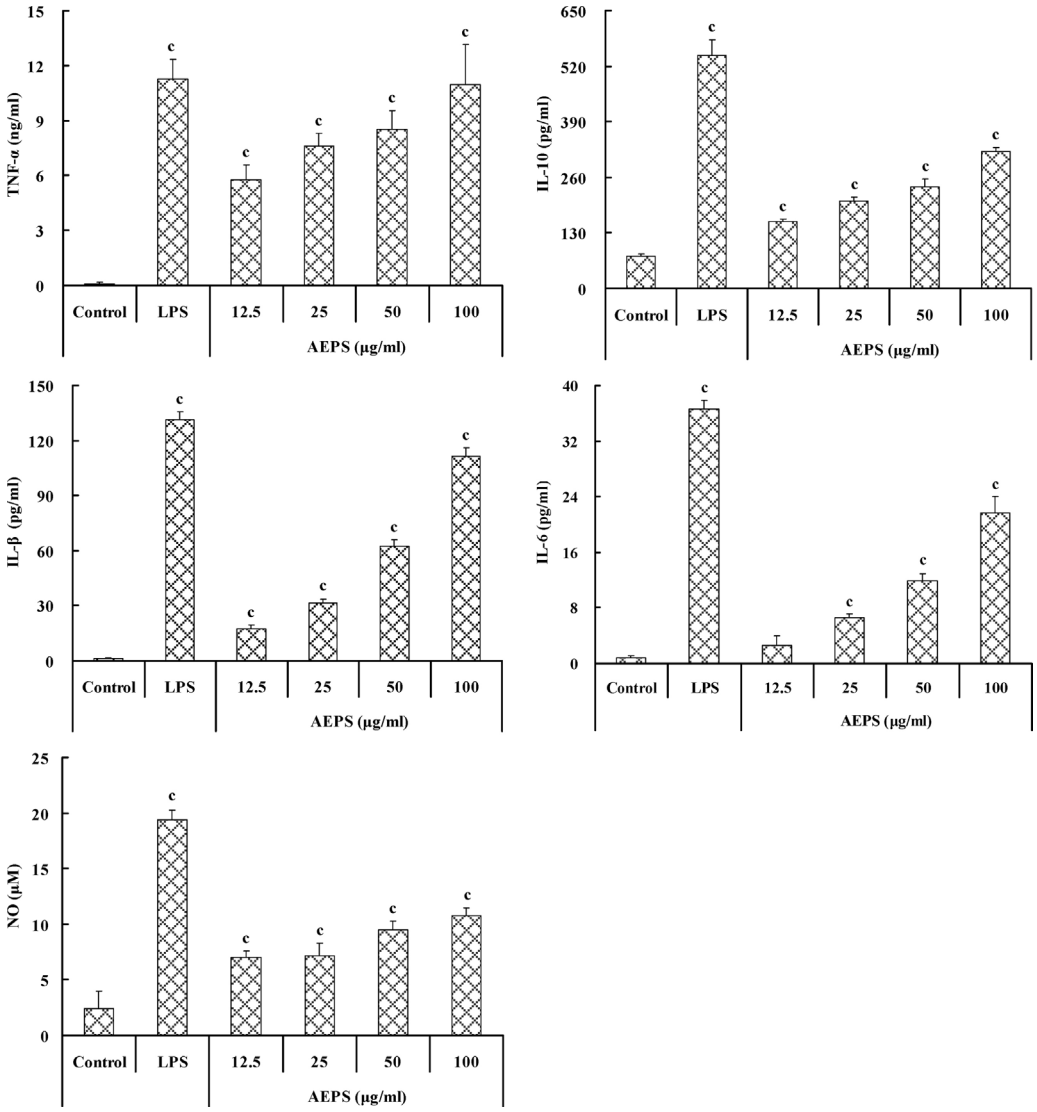

Fig. 2. Effect of the polysaccharide from the roots of *Actinidia eriantha* (AEPS) on the production of nitric oxide (NO), TNF-α, IL-1β, IL-10, and IL-6 from RAW264.7 cells. RAW264.7 cells were treated with AEPS (0–100 μg/ml) or LPS for 24 h. The values are presented as means ± SD ($n = 3$). Significant differences with control cells were designated as ^{c} $P < 0.001$.

3.4. AEPS promoted the secretion of cytokines from RAW264.7 cells

RAW264.7 cells were treated with AEPS for 24 h, and the concentrations of TNF-α, IL-1β, IL-6 and IL-10 in the supernatant was detected using ELISA reagent kit. Untreated RAW264.7 cells secrete a basal level of TNF-α and IL-10 but barely detectable amounts of IL-1β and IL-6 (Fig. 2). The addition of AEPS resulted in remarked increase in TNF-α, IL-1β, IL-6 and IL-10 protein levels in a concentration-dependent manner ($P < 0.001$).

3.5. AEPS up-regulated the expression of surface molecules on RAW264.7 cells

The expressions of CD40, CD86, CD86, MHC-I and MHC-II on RAW264.7 cells treated with AEPS for 24 h were measured by flow cytometry, and the results were shown in Fig. 3. The stimulation of RAW264.7 cells with AEPS increased the expression levels of CD40, CD86, CD86, MHC-I and MHC-II, especially CD40, CD80, and CD86.

3.6. AEPS regulated mRNA expression of inflammatory factors, chemokines and TLRs in RAW264.7 cell

Because of the prominent role of inflammatory factors, chemokines, TLR and its signaling molecules in the maturation and function of macrophages, the potentials for AEPS to regulate the expression of these mediators in RAW264.7 cells were investigated. First, the expression level of these genes in RAW264.7 cells treated with AEPS for different times were evaluated by RT-PCR. Untreated RAW264.7 cells expressed lower levels of inflammatory factors IFN-β, TNF-α, IL-1β, IL-6, IL-10, iNOS and COX-2 (Fig. 4A), and chemokines CCL-5, eotaxin, IP-10, MCP-1, MDC, MIP-1α, MIP-1β, MIP-2 and TARC (Fig. 4B). Following AEPS stimulation, the mRNA expression levels of all those inflammatory factors and chemokines significantly increased. AEPS significantly induced the mRNA expression of most examined inflammatory factors and chemokines in a time-dependent manner at the concentration of 100 μg/ml, except for IL-10, IP-10 and MIP-2 being expression peak at 2 h, 3 h, and 3 h, respectively (Fig. 4A and B). AEPS also markedly up-regulated the expression levels of TLR2, TLR9, TRIF, MyD88 and NF-κB genes in a time-dependent manner. Surprisingly, the expression levels of TLR3 and TLR4 mRNA were significantly decreased in

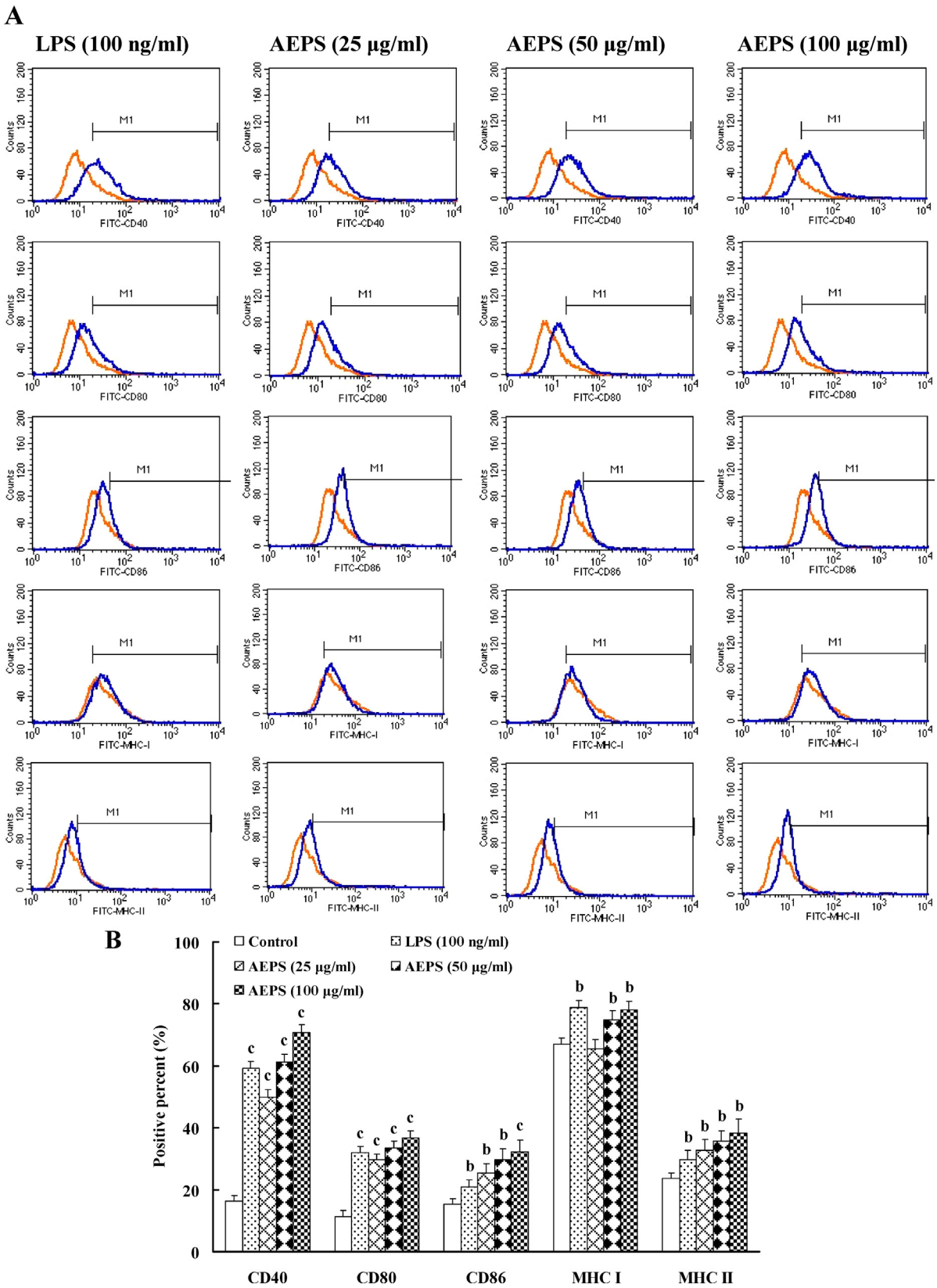

Fig. 3. Effect of the polysaccharide from the roots of *Actinidia eriantha* (AEPS) on the expression levels of surface molecules in RAW264.7 cells. RAW264.7 cells were cultured with AEPS (0–100 μg/ml) or LPS (1 μg/ml) for 24 h. (A) The expression of MHC class I, II, CD80, CD86, and CD40 was analyzed by flow cytometry. Cells in M1 gate were considered positive cells. The figure shown is representative of three independent experiments. (B) The histogram demonstrates the positive percentage of cells for various molecules in RAW264.7 cells. The values are presented as means ± SD ($n = 3$). Significant differences with control cells were designated as ^{b} $P < 0.01$ and ^{c} $P < 0.001$.

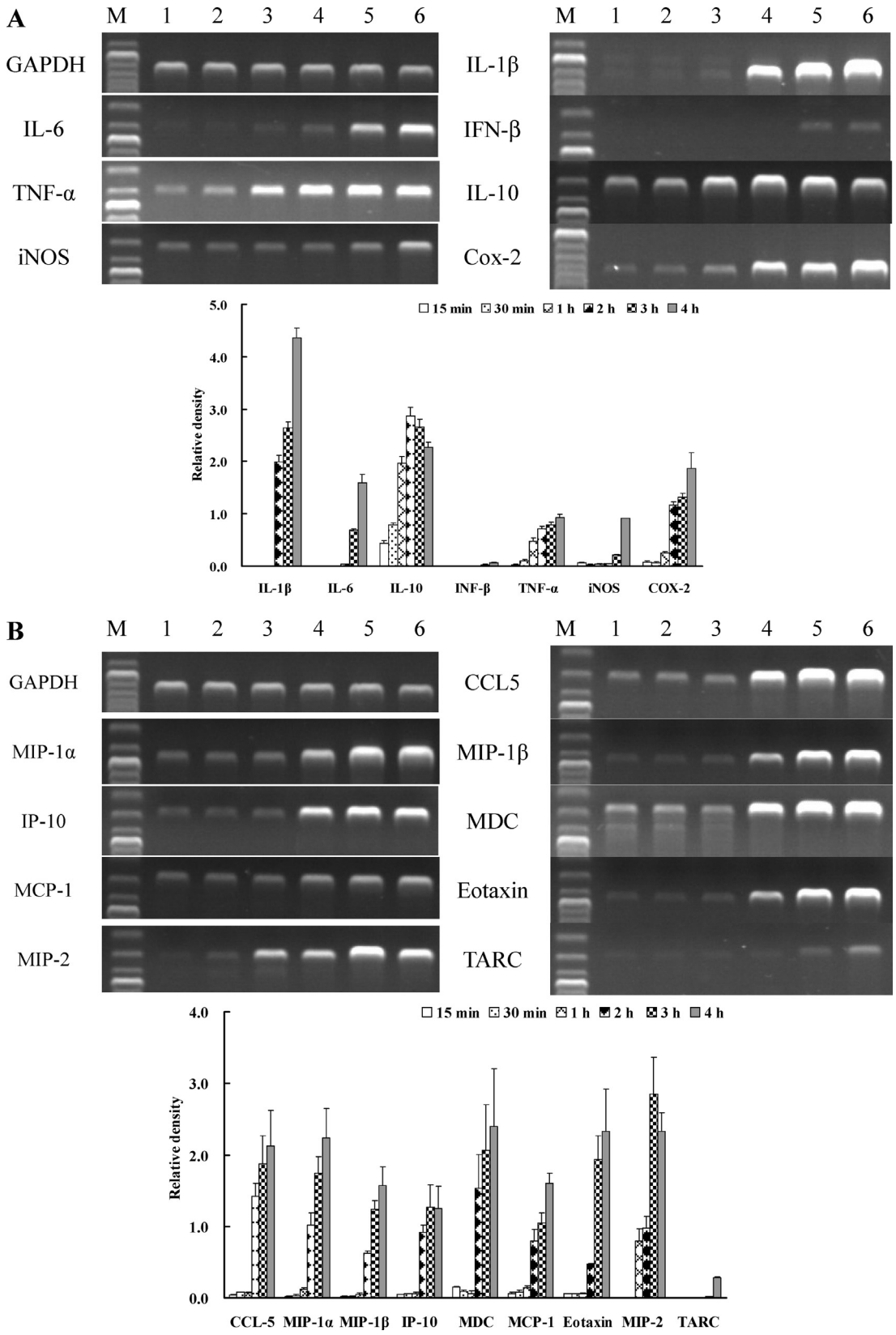

Fig. 4. The mRNA expression in RAW264.7 cells treated with AEPS (100 μg/ml). (A–C) RAW264.7 cells were incubated for 15 min, 30 min, 1 h, 2 h, 3 h, and 4 h. Lane M: DNA marker; Lane 1: 15 min; Lane 2: 30 min; Lane 3: 1 h; Lane 4: 2 h; Lane 5: 3 h; Lane 6: 4 h. (D–F) RAW264.7 cells were incubated with AEPS (0–100 μg/ml) or LPS (100 ng/ml) for 3 h. Lane M: DNA marker; Lane 1: control; Lane 2: LPS; Lane 3: AEPS 12.5 μg/ml; Lane 4: AEPS 25 μg/ml; Lane 5: AEPS 50 μg/ml; Lane 6: AEPS 100 μg/ml. The figure shown is representative of three independent experiments. The values are presented as means ± SD ($n = 3$). (A and D) cytokines; (B and E) chemokines; (C and F) TLRs and their signaling molecules.

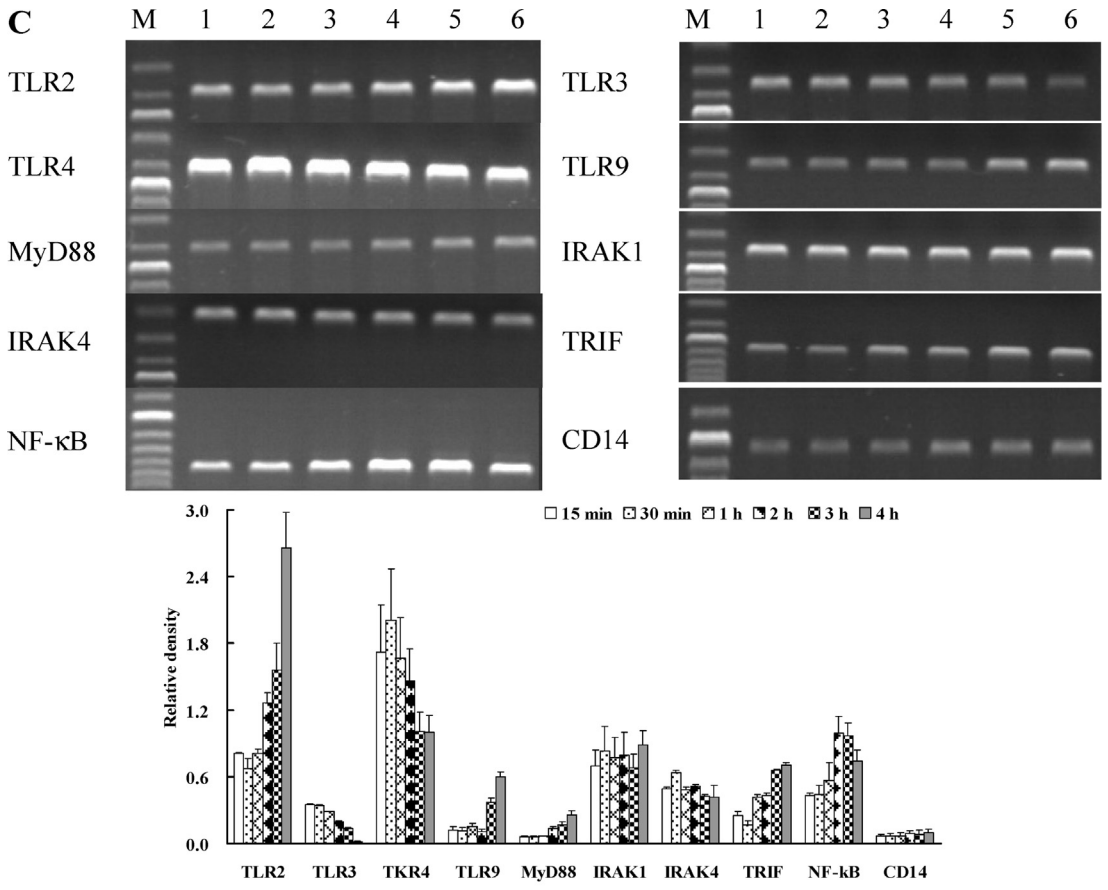

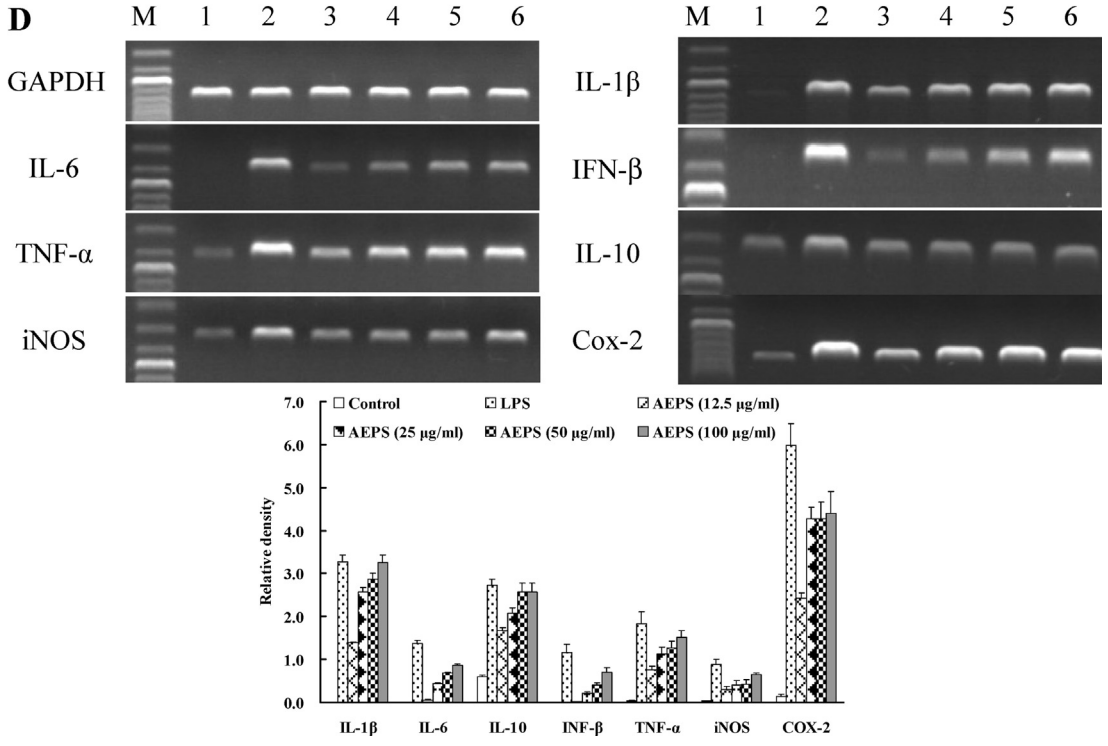

Fig. 4. (*Continued*)

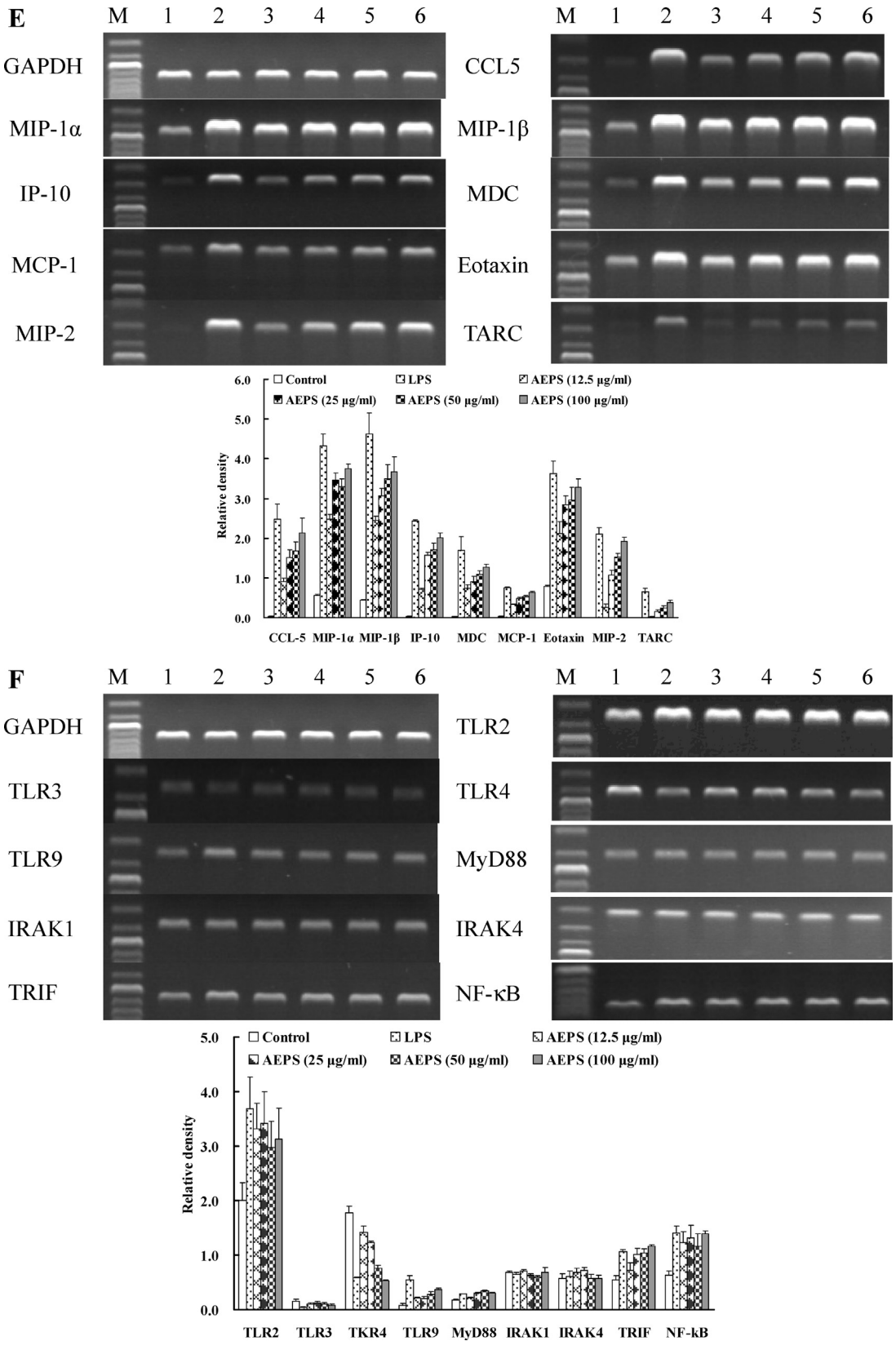

Fig. 4. (*Continued*.)

RAW264.7 cells by AEPS. In addition, AEPS had no effect on the expression levels of IRAK1, IRAK4, and CD14 genes in RAW264.7 cells (Fig. 4C).

Next, RAW264.7cells were further detected for the mRNA expression levels of the above genes after treatment with AEPS at the different concentration for 3 h. AEPS significantly up-regulated the expression levels of all tested inflammatory factor and chemokine genes in RAW264.7 cells in concentration-dependent manner (Fig. 4D and E). The mRNA expression levels of TLR2, TLR9, MyD88, TRIF and NF-κB in AEPS-treated RAW264.7 increased, but those of TLR3 and TLR4 decreased with increasing concentration of AEPS (Fig. 4F).

3.7. AEPS regulated expression of genes related to TLR signaling pathway in RAW264.7 Cells

The RT-PCR analysis revealed that AEPS could directly modulate gene expression of TLRs in RAW264.7 cells. To determine the mechanism involved in the immunomodulatory effects of AEPS on RAW264.7 cells, 84 genes central to TLR-mediated signal transduction in RAW264.7 cells were evaluated for expression using real-time PCR via TLR signaling pathway PCR array. As shown in Table 1, after treatment with AEPS, 34 genes in RAW264.7 cells exhibited significant change in mRNA expression relative to control (expression ratio showing greater than 2-fold or less than 0.5-fold difference compared with the control group). Among the differentially expressed genes, there were 28 genes up-regulated and 6 genes down-regulated.

Expressions of mRNA for TLRs including TLR2, TLR8 and TLR9 were up-regulated (2.87-, 2.80-, and 2.69-fold, respectively), whereas those of TLR3 and TLR4 were lowered significantly by 3.29- and 3.32-fold by AEPS. Transcriptional levels of effectors, adaptors and interacting proteins of TLR such as pellino 1 (PELI1), receptor (TNFRSF)-interacting serine-threonine kinase 2 (RIPK2), Toll-like receptor adaptor molecule 1 (TRIF) and interleukin-1 receptor-associated kinase 2 (IRAK2) were up-regulated (4.09-, 4.62-, 2.44-, and 2.69-fold, respectively), whereas peptidoglycan recognition protein 1 (PGLYRP1) and eukaryotic translation initiation factor 2-α kinase 2 (EIF2αK2) were down-regulated (2.53- and 2.02-fold, respectively) by AEPS.

The mRNA levels of TLR pathway downstream target genes such as IL-1β (6784.43-fold), granulocyte colony stimulating factor 3 (G-CSF, 3123.03-fold), IL-1α (921.29-fold), granulocyte-macrophage colony stimulating factor 2 (GM-CSF, 68.17-fold), IL-6 (62.75-fold), prostaglandin-endoperoxide synthase 2 (COX-2, 44.16-fold), TNF-α (16.47-fold), fibroblast interferon beta 1 (IFN-β1, 9.18-fold), chemokine (C–X–C motif) ligand 10 (CXCL10, IP-10, 8.02-fold), chemokine (C–C motif) ligand 2 (CCL2, MCP-1, 6.61-fold), lymphotoxin A (LT-α, TNF-β, 4.38-fold) and IL-10 (3.78-fold) were up-regulated after treatment with AEPS.

Transcriptional levels of several factors related to TLR downstream NF-κB pathway such as nuclear factor of κ light polypeptide gene enhancer in B-cells 1, p105 (NF-κB1, 4.33-fold), nuclear factor of κ light polypeptide gene enhancer in B-cells 2, p49/p100 (NF-κB2, 3.42-fold), nuclear factor of κ light polypeptide gene enhancer in B-cells inhibitor, alpha (IκB-α, 4.69-fold), nuclear factor of κ light polypeptide gene enhancer in B-cells inhibitor, β (IκB-β, 2.47-fold), nuclear factor of κ light polypeptide gene enhancer in B-cells inhibitor-like 1 (IκB-L, 2.63-fold), reticuloendotheliosis oncogene (REL, 3.64-fold) and tumor necrosis factor, α-induced protein 3 (TNFαIP3, A20, 26.95-fold) was up-regulated in AEPS-treated RAW264.7 cells. Interestingly, AEPS relatively less altered the expression of the genes associated with other TLR downstream pathway such as JNK/p38 pathway, NF/IL6 pathway and IRF pathway in the array by 2-fold or more. JNK/p38 pathway: expression of mitogen-activated protein kinase kinase kinase 1 (MAP3K1, MEKK1) was down-regulated by 4.11-fold upon AEPS treatment. NF/IL6 pathway: C-type lectin domain family 4, member e (CLEC4E), which is a macrophage-inducible C-type lectin involved in infection and inflammation, expression was up-regulated by 3.49-fold. IRF pathway: Interferon regulatory factor 1 (IRF1) expression was reduced by 3.35-fold. In addition, the mRNA level for CD80 antigen involved in regulation of adaptive immunity was up-regulated by AEPS (3.33-fold). AEPS, therefore, may exert the immunomodulatory effect on RAW264.7 cells through altering the expression levels of these genes.

3.8. Validation of Toll-like receptor signaling pathway PCR array results by RT-PCR

To confirm the validity of the PCR array results, semi-quantitative RT-PCR was undertaken for 12 putative differentially expressed genes including 10 up-regulated genes and 2 down-regulated genes. As shown in Fig. 5, after treatment with AEPS, the mRNA expression levels of CCL-2, COX-2, CXCL10, IFN-β, IL-1β, IL-6, TNF-α, TLR2, TLR8 and TLR9 were increased, whereas those of TLR3 and TLR4 were decreased in RAW264.7 cells compared with the control. Differential expression of selected genes was considered to be validated as the similar results between RT-PCR and PCR array data.

3.9. AEPS induced the IκB-α degradation and NF-κB activation in RAW264.7 cells

NF-κB is an important transcription factor to regulate proinflammatory mediators in activated macrophages. The signals originated from TLR are known to activate NF-κB. To investigate whether AEPS activated the NF-κB signaling pathway, RAW264.7 cells were treated with AEPS for 30 min, and then the cytoplasmic level of IκB-α and nuclear level of NF-κB p65 subunit were analyzed by Western blot. As shown in Fig. 6A, AEPS induced the IκB-α degradation in cytosol and the translocation of NF-κB p65 subunit into the nucleus of RAW264.7 cells. These results indicated AEPS could induce NF-κB activation in macrophages. To convincingly demonstrate the specificity of NF-κB activation by AEPS, the effects of PDTC, an inhibitor of NF-κB, was investigated using RT-PCR. PDTC inhibited the IL-1β mRNA expression induced by AEPS in RAW 264.7 cells (Fig. 6B), confirming the involvement of NF-κB in the activation of RAW264.7 cells by AEPS.

4. Discussion

AEPS has previously been proved to possess the immunological adjuvant effect and antitumor activity through improving immune response. However, its molecular mechanism responsible for regulating immune response is not fully understood. In the present study the activation of AEPS on the macrophages was investigated and its subsequent intracellular signaling pathways were explored using RAW264.7 macrophage as a cellular model.

One of the most distinguished features of macrophage activation would be an increase in pinocytic and phagocytic activity. Therefore, the effects of AEPS on the pinocytic activity and phagocytic uptake of RAW264.7 cells were first determined using neutral red assay and flow cytometer, respectively. The results suggested AEPS could prime macrophages for an enhanced pinocytic activity and phagocytic capacities.

Macrophages actively participate in immune responses by releasing proinflammatory cytokines (TNF-α and IL-1β) and inflammatory factors such as NO (Duerksen-Hughes et al., 1992; Farias-Eisner, Sherman, Aeberhard, & Chaudhuri, 1994; Lorsbach, Murphy, Lowenstein, Snyder, & Russell, 1993). In this study, AEPS significantly increased the production of TNF-α, IL-1β, IL-6 and

Table 1
Genes found to be up-regulated or down-regulated by the polysaccharide from the roots of *Actinidia eriantha* (AEPS) in RAW264.7 cells based on PCR array.

Functional Gene groups		Symbol	UniGene	RefSeq	Description	Fold
Toll-Like Receptors	TLR2	Mm.87596	NM_011905	Toll-like receptor 2	2.87	
	TLR3	Mm.33874	NM_126166	Toll-like receptor 3	−3.29	
	TLR4	Mm.38049	NM_021297	Toll-like receptor 4	−3.32	
	TLR8	Mm.196676	NM_133212	Toll-like receptor 8	2.8	
	TLR9	Mm.44889	NM_031178	Toll-like receptor 9	2.69	
Adaptors, TLR interacting proteins and effectors	PELI1	Mm.28957	NM_023324	Pellino 1	4.09	
	PGLYRP1	Mm.21855	NM_009402	Peptidoglycan recognition protein 1	−2.53	
	RIPK2 (CARD3)	Mm.112765	NM_138952	Receptor (TNFRSF)-interacting serine-threonine kinase 2	4.62	
	TICAM-1 (TRIF)	Mm.203952	NM_174989	Toll-like receptor adaptor molecule 1	2.44	
	IRAK-2	Mm.152142	NM_172161	Interleukin-1 receptor-associated kinase 2	2.69	
	EIF2αK2 (PKR)	Mm.378990	NM_011163	Eukaryotic translation initiation factor 2-alpha kinase 2	−2.02	
TLR downstream target genes	CCL2 (MCP-1)	Mm.290320	NM_011333	Chemokine (C-C motif) ligand 2	6.61	
	CSF2 (GM-CSF)	Mm.4922	NM_009969	Colony stimulating factor 2 (granulocyte-macrophage)	68.17	
	CSF3 (G-CSF)	Mm.1238	NM_009971	Colony stimulating factor 3 (granulocyte)	3123.03	
	CXCL10	Mm.877	NM_021274	Chemokine (C-X-C motif) ligand 10	8.02	
	IFN-β1	Mm.1245	NM_010510	Interferon beta 1, fibroblast	9.18	
	IL-1α	Mm.15534	NM_010554	Interleukin 1 alpha	921.29	
	IL-1β	Mm.222830	NM_008361	Interleukin 1 beta	6784.43	
	IL-6	Mm.1019	NM_031168	Interleukin 6	62.75	
	IL-10	Mm.874	NM_010548	Interleukin 10	3.78	
	PTGS2 (COX-2)	Mm.292547	NM_011198	Prostaglandin-endoperoxide synthase 2	44.16	
	LT-α (TNF-β)	Mm.87787	NM_010735	Lymphotoxin A	4.38	
	TNF-α	Mm.1293	NM_013693	Tumor necrosis factor	16.47	
TLR downstream pathway	NF-κB Pathway	NF-κB1	Mm.256765	NM_008689	Nuclear factor of kappa light polypeptide gene enhancer in B-cells 1, p105	4.33
		NF-κB2	Mm.102365	NM_019408	Nuclear factor of kappa light polypeptide gene enhancer in B-cells 2, p49/p100	3.42
		IκB-a	Mm.170515	NM_010907	Nuclear factor of kappa light polypeptide gene enhancer in B-cells inhibitor, alpha	4.69
		IκB-b	Mm.220333	NM_010908	Nuclear factor of kappa light polypeptide gene enhancer in B-cells inhibitor, beta	2.47
		IκB-L	Mm.300795	NM_010909	Nuclear factor of kappa light polypeptide gene enhancer in B-cells inhibitor-like 1	2.63
		REL	Mm.4869	NM_009044	Reticuloendotheliosis oncogene	3.64
		TNFAIP3 (A20)	Mm.116683	NM_009397	Tumor necrosis factor, alpha-induced protein 3	26.95
	JNK/p38 Pathway	MAP3K1 (MEKK1)	Mm.15918	NM_011945	Mitogen-activated protein kinase kinase kinase 1	−4.11
	IRF Pathway	IRF1	Mm.105218	NM_008390	Interferon regulatory factor 1	−3.35
	NF/IL6 Pathway	CLEC4E	Mm.248327	NM_019948	C-type lectin domain family 4, member e	3.49
Regulation of adaptive immunity		CD80	Mm.89474	NM_009855	CD80 antigen	3.33

Gene alterations after AEPS-exposedRAW264.7 cells were analyzed using quantitative real time PCR profiling. Only signals that differed from untreated cells by at least 2 fold were considered as significant. Changes are indicated as (+) up-regulation and (−) down-regulation as compared to control group.

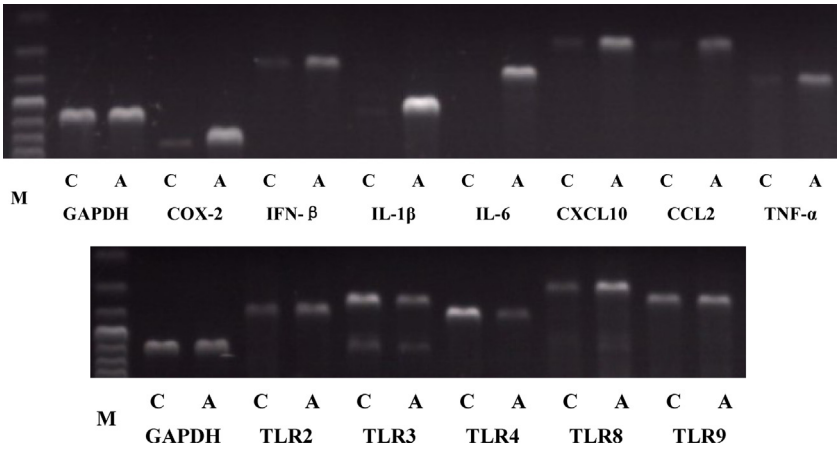

Fig. 5. RT-PCR validation of PCR array results. After cells were treated by 50 μg/ml AEPS for 3 h, expression changes of 12 genes which were up-regulated (COX-2, IFN-β, IL-1β, IL-6, CXCL10, CCL2, TNF-α, TLR2, TLR8, and TLR9) or down-regulated (TLR3 and TLR4) in PCR array analysis detected by RT-PCR using specific primers as described in the text. The housekeeping gene GAPDH was used as endogenous control. The figures shown were representative of three independent experiments.

IL-10, promoted the secretion of NO, and up-regulated the mRNA expression levels of TNF-α, IL-1β, IL-6, IL-10, iNOS and COX-2 in RAW264.7 cells (Figs. 2 and 4), further indicating that AEPS effectively activated macrophages.

Activation of T cell generally requires a signal delivered via interaction of the TCR with specific antigen on MHC molecules (MHC-I and MHC-II) and costimulatory molecules such as CD80, CD86 and CD40 (Van Gool, Vandenberghe, de Boer, & Ceuppens, 1996). FACS analysis showed that AEPS significantly induced the expression of accessory and costimulatory molecules MHC-I, MHC-II, CD80, CD86, and CD40 on RAW264.7 cells (Fig. 3).

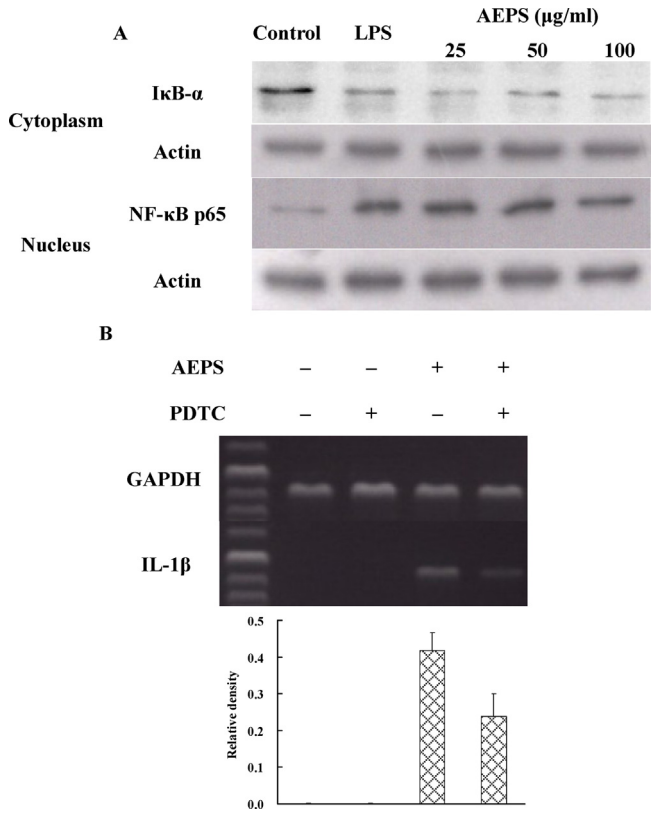

Fig. 6. Roles of NF-κB pathways in activation of macrophages by AEPS. (A) RAW264.7 cells were treated with AEPS (0–100 μg/ml) or LPS (100 ng/ml) for 30 min, and NF-κB p65 in nuclear extract and IκB-α in cytosolic extract were detected by Western blot. (B) RAW 264.7 cells were pretreated with or without 15 μM PDTC for 30 min and followed by stimulation with medium or AEPS (50 μg/ml) for 3 h, and the expression levels of IL-1β and GAPDH mRNA were determined using RT-PCR. The figure shown is representative of three independent experiments. The values are presented as means ± SD ($n = 3$).

The differential chemokine and cytokine production is a key feature of activated and polarized macrophage. The cytokines associated with polarized type I responses of activated M1 phenotypes include IL-12 and TNF-α. In contrast, M2 cells typically produce IL-10 (Rauh et al., 2005). Differential production of chemokines integrates M1 and M2 macrophage in circuits of amplification to attract Th1 and Th2 or T regulatory (Treg) cells for inducing polarized T cell responses (Mantovani, Sozzani, Locati, Allavena, & Sica, 2002). During macrophage activation, distinct repertoires of inflammatory chemokines such as macrophage inflammatory protein (MIP)-1α, MIP-1β, regulated on activation normal T cell expressed and secreted (RANTES/CCL5) (Dorner et al., 2002), and IFN-inducible protein-10 (IP-10) are expressed during polarized type I response. Similarly, thymus and activation-related chemokine (TARC), macrophage-derived chemokine (MDC), eotaxin-2, monocyte chemotactic protein-1 (MCP-1), and major intrinsic protein-2 (MIP-2) are found to be associated with polarized type II response (Mantovani et al., 2004). AEPS remarkably induced not only the expression of M1 chemokines CCL-5, MIP-1α, MIP-1β and IP-10, but M2 chemokines eotamin-2, MDC, MCP-1, MIP-2 and TARC. As the above discussed, AEPS significantly promoted the production of TNF-α and IL-10 from RAW264.7 cells. All these results suggested M1 and M2 balances of AEPS-activated RAW264.7 cells, and implicated that AEPS would simultaneously induces Th1 and Th2-type response, which was consistent with that AEPS elicited a balanced Th1/Th2 response to OVA in mice (Sun et al., 2009).

TLRs were identified as important membrane receptors involved in the activation of macrophages. Engagement of TLRs by pathogen-associated molecular patterns (PAMPs) on cells triggers the signaling pathways that drive the innate immune effector functions and lead to initiate and strengthen adaptive immunity through induction of interleukins and the costimulatory molecules (Pasare & Medzhitov, 2004). It has been postulated that TLRs are involved in regulating the effect of immune adjuvants (Medzhitov, Preston-Hurlburt, & Janeway, 1997). Recently, there have been several reports demonstrating TLR-dependent activation of macrophages by polysaccharides, and it was suggested that TLR has a relatively broad specificity to polysaccharides isolated from a variety of sources (Petrovsky & Cooper, 2011). Therefore, the study on AEPS-mediated enhancement of the expression of TLR and its

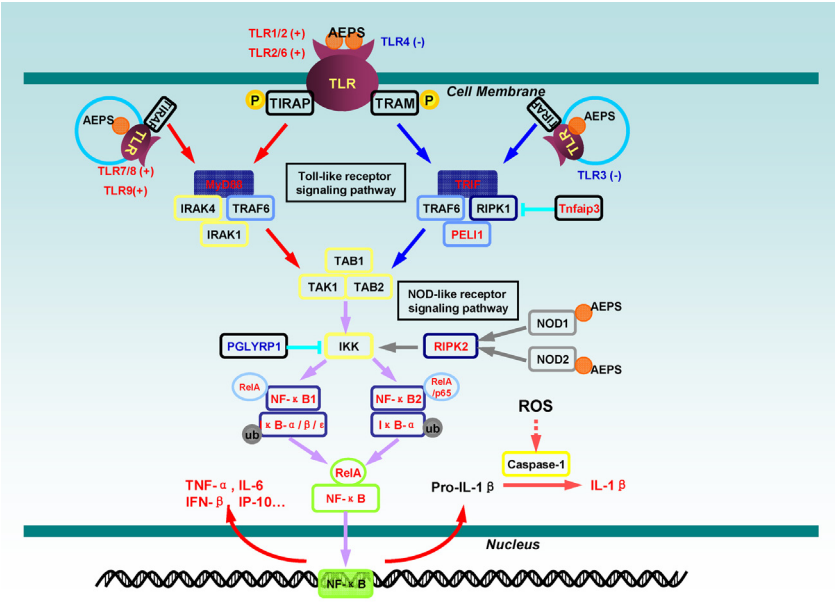

Fig. 7. Possible signaling pathway in RAW264.7 cells activated by AEPS. Genes modulated in RAW264.7 cells after AEPS exposure along the TLRs/NF-κB signaling pathway were represented in red (up), green (down) and black (no change/untested). (For interpretation of the references to color in this figure legend, the reader is referred to the web version of this article.)

signaling molecules in RAW264.7 cells would help to understand its molecular mechanism of immunomodulatory action. RT-PCR analysis showed that AEPS directly significantly up-regulated the mRNA expression levels of some TLRs such as TLR2, TLR8 and TLR9 and its signaling molecules including MyD88 and TRIF in RAW264.7. Surprisingly, the mRNA expression level of TLR3 and TLR4 decreased with increasing concentration of AEPS. Similar results concerning about TLR4 expression in macrophages were observed following LPS and CpG DNA stimulation (An et al., 2002). The un-inducibility of TLR4 might be due to its higher expression level in un-stimulated RAW264.7 cells. It was also reported that LPS treatment results in down-regulation of TLR4 expression on RAW264.7 cells (Rhule, Navarro, Smith, & Shepherd, 2006) and mouse peritoneal macrophages (Akashi et al., 2000) measured by flow cytometry.

To further insight into the molecular mechanism on immunomodulatory action of AEPS, RT^2 Profiler Mouse TLR Signaling Pathway PCR Array was selected for exploring the effect of AEPS on genes related to TLR-mediated signal transduction in RAW264.7 cells. This array easily and reliably profiles the expression of 84 genes central to TLR-mediated signal transduction, including members of the TLRs and their adaptor and effector proteins as well as the members of TLR downstream NFκB, JNK/p38, IRF, and NF/IL6 signaling pathways (Luo, Wang, & Jin, 2012). The differentially expressed genes in RAW264.7cells induced by AEPS included 28 up-regulated and 6 down-regulated genes. This PCR Array results were further verified by RT-PCR assay.

The PCR Array data presented in this study demonstrated that the treatment of RAW264.7 cells with AEPS up-regulated the mRNA expression level of TLR2, TLR8 and TLR9, whereas down-regulated that of TLR3 and TLR4, which was consistent with the above results by RT-PCR. TLRs act alone or as heterodimers, interacting with adaptor proteins to initiate MyD88-Dependent or/and TRIF-dependent (MyD88-independent) responses (Beutler, Hoebe, Du, & Ulevitch, 2003). As to effectors, adaptors and interacting proteins of TLRs, the expression levels of PELI1, RIPK2, TRIF (TIKAM1) and IRAK2 were increased, and those of PGLYRP1 and EIF2αAK2 were lowered in RAW264.7 cells after AEPS treatment, respectively. Among them, PELIl and TRIF involved in TRIF-dependent pathway, while IRAK2 in MyD88-dependent response. PELI1 is an E3 ubiquitin ligase needed for the transmission of TRIF-dependent TLR signals and facilitates TRIF-dependent TLR signaling and proinflammatory cytokine production (Chang, Jin, & Sun, 2009). PGLYRP1 suppress a pro-inflammatory response by negatively mediating TLR2 and NF-κB pathway (Sun, Chang, Le, & Shi, 2008). These results suggested that AEPS could act through both MyD88- and TRIF-dependent TLR signal pathways. RIPK2 is a member of the caspase-associated recruitment domain (CARD) protein family and the first reported NF-κB-dependent protein kinase that positively regulates NF-κB activity. Among CARD genes, CARD6, nucleotide-binding oligomerization domain-containing protein 1 (NOD1), and NOD2 were reported to induce the activation of NF-κB through associating with RIPK2 (Chang, Chen, & Nie, 2010; Dufner, Pownall, & Mak, 2006; Kobayashi et al., 2002). RIPK2 promotes NF-κB function via interaction with IKK-γ (Yin, Krikorian, Logan, & Csizmadia, 2010). EIF2αK2 (also known as PKR or PRKR) is not only an effector molecule on the cellular response to double-stranded RNA (Meurs et al., 1990), it but also integrates signals in response to TLR activation, growth factors, and diverse cellular stresses (Garcia et al., 2006). PKR physically interacts with several inflammasome components, including NOD-like receptor (NLR) family pyrin domain-containing 3 (NLRP3), NLRP1, NLR family CARD domain-containing protein 4 (NLRC4), absent in melanoma 2 (AIM2), and broadly regulates inflammasome activation. PKR autophosphorylation in a cell-free system with recombinant NLRP3, apoptosis-associated speck-like protein containing a CARD (ASC) and pro-caspase-1 reconstitutes inflammasome activity (Lu et al., 2012). Therefore, in addition to TLR signaling pathway, NOD/RIP2 signaling networks could involve in the wide range of cytokines and chemokines induced by AEPS in RAW264.7 cells.

Several proinflammatory factors such as IL-1β, G-CSF, IL-1α, GM-CSF, IL-6, COX-2, TNF-α, IFN-β, IP-10 (CXCL10), MCP-1 (CCL2), TNF-β and IL-10 were also significantly up-regulated after treatment with AEPS. These results are consistent with the above results by RT-PCR. The wide range of cytokines and chemokines in RAW264.7 cells induced by AEPS raises interesting questions about the cell signaling pathways activated.

Upon activation, TLRs activate two major signaling pathways transcription factor NF-κB and the mitogen-activated protein kinases (MAPKs). NF-κB is a pleiotropic regulator of many genes involved in immune response, controls the expression of proinflammatory genes such as cytokines, adhesion molecules and cytotoxic molecule-generating enzymes including iNOS and COX-2 (Xie, Kashiwabara, & Nathan, 1994). PCR array results showed that the genes involved in the TLR downstream NF-κB signal pathway such as NF-κB1, NF-κB2, IκB-α, IκB-β, IκB-L, REL and TNFAIP3 (A20) in RAW264.7 cells were up-regulated by AEPS. Noteworthy, TNFAIP3 (A20), an intracellular ubiquitin-editing protein, is a key player in the negative feedback regulation of NF-kB signaling in response to multiple stimuli (Vereecke, Beyaert, & van Loo, 2009). TNFAIP3 was up-regulated, which likely assisted in the prevention of NF-κB over-activation in this study. On the other hand, MAPKs, including extracellular signal-regulated kinase (ERK), *c*-Jun *N*-terminal kinase (JNK) and p38 MAPK, also plays an important role in signal transduction pathways and regulates cytokine release (Johnson & Lapadat, 2002). Interestingly, AEPS relatively less altered the expression of the genes associated with JNK/p38 pathway. Among eight genes involved in JNK/p38 pathway such as ELK1, FOS, JUN, MAP2K3 (MKK3), MAP2K4 (MKK4), MAP3K1 (MEKK1), MAPK8 (JNK1), MaAPK9 (JNK2), only MAP3K1 (MEKK1) was altered upon AEPS treatment, with being down-regulated by 4.11-fold. It seems to indicate that MAPKs are not involved in the immunomodulatory effect of AEPS on macrophages.

In order to further unravel the mechanisms involved in AEPS-induced macrophage activation, the effect of AEPS on the translocation of NF-κB was examined by Western blot analysis using an I-κBα and NF-κB subunit p65 antibody. In our studies, AEPS remarkably promoted cytoplasmic IκB-α degradation and increased nuclear levels of the NF-κB p65 subunit in RAW264.7 cells (Fig. 6). In addition, PDTC inhibited IL-1β mRNA expression in RAW 264.7 cells induced by AEPS. These results suggested that the activity of AEPS was dependent on the activation of NF-κB signaling pathways. In conclusion, AEPS activated macrophages and elicited a M1 and M2 response in RAW264.7 cells through TLRs/NF-κB signaling pathway (Fig. 7). For the first time, we have established the regulation of multiple TLRs and their associated signaling genes following activation of RAW264.7 cells by AEPS. These data further expand current knowledge on mechanism how AEPS acts as potent adjuvant and antitumor agent with immunomodulatory activity.

Acknowledgments

This work was supported by Grant-in-Aid from the National Natural Science Foundation of China (no. 31272597), the Zhejiang Provincial Natural Science Foundation of China (no. R3080027), the National Key Project of Scientific and Technical Supporting Programs Funded by Ministry of Science & Technology of China (no. 2008BADB4B06-2), the Key Scientific and Technological Innovation Team of Zhejiang Province (no. 2010R50031-13), Chinese Universities Scientific Fund (no. 2010KLEP007), and the Fundamental Research Funds for the Central Universities (no. 2012FZA6017). PCR array analysis was performed by Kangchen Bio-tech, Shanghai, China.

References

Akashi, S., Shimazu, R., Ogata, H., Nagai, Y., Takeda, K., Kimoto, M., et al. (2000). Cutting edge: Cell surface expression and lipopolysaccharide signalling via the Toll-like receptor 4-MD-2 complex on mouse peritoneal macrophages. *The Journal of Immunology*, *164*, 3471–3475.

An, H. Z., Xu, H. M., Yu, Y. Z., Zhang, M. H., Qi, R. Z., Yan, X. Y., et al. (2002). Up-regulation of TLR9 gene expression by LPS in mouse macrophages via activation of NF-(B, ERK and p38 MAPK signal pathways. *Immunology Letters*, *81*, 165–169.

Beutler, B. (2004). Innate immunity: An overview. *Molecular Immunology*, *40*, 845–859.

Beutler, B., Hoebe, K., Du, X., & Ulevitch, R. J. (2003). How we detect microbes and respond to them: The toll-like receptors and their transducers. *Journal of Leukocyte Biology*, *74*, 479–485.

Chang, M., Jin, W., & Sun, S. C. (2009). Peli1 facilitates TRIF-dependent Toll-like receptor signalling and proinflammatory cytokine production. *Nature Immunology*, *10*, 1089–1095.

Chang, M. X., Chen, W. Q., & Nie, P. (2010). Structure and expression pattern of teleost caspase recruitment domain (CARD) containing proteins that are potentially involved in NF-kB signalling. *Development and Comparative Immunology*, *34*, 1–13.

Chen, F. Y., Ni, Y., Ye, Y. P., Sun, H. X., Li, X. Y., & Xu, S. F. (2012). Stephanthraniline A inhibits the proliferation and activation of T cells in vitro and in vivo. *European Journal of Pharmacology*, *685*, 186–197.

Cheng, A. W., Wan, F. C., Wang, J. Q., Jin, Z. Y., & Xu, X. M. (2008). Macrophage immunomodulatory activity of polysaccharides isolated from *Glycyrrhiza uralensis* fish. *International Immunopharmacology*, *8*, 43–50.

Dorner, B. G., Scheffold, A., Rolph, M. S., Huser, M. B., Kaufmann, S. H. E., Radbruch, A., et al. (2002). MIP-1α, MIP-1β, RANTES, and ATAC/lymphotactin function together with IFN-(as type 1 cytokines. *Proceedings of the National Academy of Sciences of the United States of America*, *99*, 6181–6186.

Duerksen-Hughes, P. J., Day, D. B., Laster, S. M., Zachariades, N. A., Aquino, L., & Gooding, L. R. (1992). Both tumor necrosis factor and nitric oxide participate in lysis of simian virus 40-transformed cells by activated macrophages. *Journal of Immunology*, *149*, 2114–2122.

Dufner, A., Pownall, S., & Mak, T. W. (2006). Caspase recruitment domain protein 6 is a microtubule-interacting protein that positively modulates NF-κB activation. *Proceedings of the National Academy of Sciences of the United States of America*, *103*, 988–993.

Farias-Eisner, R., Sherman, M. P., Aeberhard, E., & Chaudhuri, G. (1994). Nitric oxide is an important mediator for tumoricidal activity in vivo. *Proceedings of the National Academy of Sciences of the United States of America*, *91*, 9407–9411.

Garcia, M. A., Gil, J., Ventoso, I., Guerra, S., Domingo, E., Rivas, C., et al. (2006). Impact of protein kinase PKR in cell biology: From antiviral to antiproliferative action. *Microbiology and Molecular Biology Reviews*, *70*, 1032–1060.

Granell, A., Fernández-del-Carmen, A., & Orzáez, D. (2010). In planta production of plant-derived and non-plant-derived adjuvants. *Expert Review of Vaccines*, *9*, 843–858.

Hartley, J. W., Evans, L. H., Green, K. Y., Naghashfar, Z., Macias, A. R., Zerfas, P. M., et al. (2008). Expression of infectious murine leukemia viruses by RAW264.7 cells, a potential complication for studies with a widely used mouse macrophage cell line. *Retrovirology*, *5*, 1–6.

Johnson, G. L., & Lapadat, R. (2002). Mitogen-activated protein kinase pathways mediated by ERK, JNK and p38 protein kinases. *Science*, *298*, 1911–1912.

Kobayashi, K., Inohara, N., Hernandez, L. D., Galán, J. E., Núñez, G., Janeway, C. A., et al. (2002). RICK/Rip2/CARDIAK mediates signalling for receptors of the innate and adaptive immune systems. *Nature*, *416*, 194–199.

Licciardi, P. V., & Underwood, J. R. (2011). Plant-derived medicines: A novel class of immunological adjuvants. *International Immunopharmacology*, *11*, 390–398.

Lorsbach, R. B., Murphy, W. J., Lowenstein, C. J., Snyder, S. H., & Russell, S. W. (1993). Expression of the nitric oxide synthase gene in mouse macrophages activated for tumor cell killing. Molecular basis for the synergy between interferon-gamma and lipopolysaccharide. *Journal of Biological Chemistry*, *268*, 1908–1913.

Lu, B., Nakamura, T., Inouye, K., Li, J. H., Tang, Y. T., Lundbäck, P., et al. (2012). Novel role of PKR in inflammasome activation and HMGB1 release. *Nature*, *488*, 670–674.

Luo, W., Wang, C. Y., & Jin, L. (2012). Baicalin downregulates *Porphyromonas gingivalis* lipopolysaccharide-upregulated IL-6 and IL-8 expression in human oral keratinocytes by negative regulation of TLR signalling. *PLoS One*, *7*, e51008.

Mantovani, A., Sozzani, S., Locati, M., Allavena, P., & Sica, A. (2002). Macrophage polarization: Tumor-associated macrophages as a paradigm for polarized M2 mononuclear phagocytes. *Trends in Immunology*, *23*, 549–555.

Mantovani, A., Sica, A., Sozzani, S., Allavena, P., Vecchi, A., & Locati, M. (2004). The chemokine system in diverse forms of macrophage activation and polarization. *Trends in Immunology*, *25*, 677–686.

Medzhitov, R., Preston-Hurlburt, P., & Janeway, C. A., Jr. (1997). A human homologue of the *Drosophila* toll protein signals activation of adaptive immunity. *Nature*, *388*, 394–397.

Meurs, E., Chong, K., Galabru, J., Thomas, N. S., Kerr, I. M., Williams, B. R., et al. (1990). Molecular cloning and characterization of the human doublestranded RNA-activated protein kinase induced by interferon. *Cell*, *62*, 379–390.

Pasare, C., & Medzhitov, R. (2004). Toll-like receptors and acquired immunity. *Seminars in Immunology*, *16*, 23–26.

Petrovsky, N., & Cooper, P. D. (2011). Carbohydrate-based immune adjuvants. *Expert Review of Vaccines*, *10*, 523–537.

Rauh, M. J., Ho, V., Pereira, C., Sham, A., Sly, L. M., Lam, V., et al. (2005). SHIP represses the generation of alternatively activated macrophages. *Immunity*, *23*, 361–374.

Rhule, A., Navarro, S., Smith, J. R., & Shepherd, D. M. (2006). *Panax notoginseng* attenuates LPS-induced pro-inflammatory mediators in RAW264.7 cells. *Journal of Ethnopharmacology*, *106*, 121–128.

Sun, H. X., Wang, H., Xu, H. S., & Ni, Y. (2009). Novel polysaccharide adjuvant from the roots of *Actinidia eriantha* with dual Th1 and Th2 potentiating activity. *Vaccine*, *27*, 3984–3991.

Sun, J., Chang, G. F., Le, G. W., & Shi, Y. H. (2008). Building of *Lactobacillus* peptidoglycan specific immune modulating pathway by text-miming approach. *Chinese Journal of Microecology*, *20*, 1–6.

Van Gool, S. W., Vandenberghe, P., de Boer, M., & Ceuppens, J. L. (1996). CD80, CD86 and CD40 provide accessory signals in a multiple-step T-cell activation model. Immunological. *Reviews*, *153*, 47–83.

Vereecke, L., Beyaert, R., & van Loo, G. (2009). The ubiquitin-editing enzyme A20 (TNFAIP3) is a central regulator of immunopathology. *Trends in Immunology*, *30*, 383–391.

Wang, J. J., Chen, X. F., Zhou, Z. H., Li, J. H., & Sun, H. X. (2013). The inhibitory effect of 3(-hydroxy-12-oleanen-27-oic acid on growth and motility of human hepatoma HepG2 cells through JNK and Akt signalling pathway. In *Evidence-Based Complementary and Alternative Medicine*. Article ID 685159, 17 pages

Xie, Q. W., Kashiwabara, Y., & Nathan, C. (1994). Role of transcription factor NF-κB/Rel in induction of nitric oxide synthase. *Journal of Biological Chemistry*, *269*, 4705–4708.

Xu, H. S., Yao, L., Sun, H. X., & Wu, Y. W. (2009). Chemical composition and anti-tumor activity of different polysaccharides from the roots of *Actinidia eriantha*. *Carbohydrate Polymers*, *78*, 316–322.

Yin, X. X., Krikorian, P., Logan, T., & Csizmadia, V. (2010). Induction of RIP-2 kinase by proinflammatory cytokines is mediated via NF-κB signalling pathways and involves a novel feed-forward regulatory mechanism. *Molecular and Cellular Biochemistry*, *333*, 251–259.